

# Image Change Detection Algorithms: A Systematic Survey

Richard J. Radke, *Member, IEEE*, Srinivas Andra, *Student Member, IEEE*, Omar Al-Kofahi, and  
Badrinath Roysam, *Member, IEEE, Student Member, IEEE*

**Abstract**—Detecting regions of change in multiple images of the same scene taken at different times is of widespread interest due to a large number of applications in diverse disciplines, including remote sensing, surveillance, medical diagnosis and treatment, civil infrastructure, and underwater sensing. This paper presents a systematic survey of the common processing steps and core decision rules in modern change detection algorithms, including significance and hypothesis testing, predictive models, the shading model, and background modeling. We also discuss important preprocessing methods, approaches to enforcing the consistency of the change mask, and principles for evaluating and comparing the performance of change detection algorithms. It is hoped that our classification of algorithms into a relatively small number of categories will provide useful guidance to the algorithm designer.

**Index Terms**—Background modeling, change detection, change mask, hypothesis testing, illumination invariance, mixture models, predictive models, shading model, significance testing.

## I. INTRODUCTION

**D**ETECTING regions of change in images of the same scene taken at different times is of widespread interest due to a large number of applications in diverse disciplines. Important applications of change detection include video surveillance [1]–[3], remote sensing [4]–[6], medical diagnosis and treatment [7]–[11], civil infrastructure [12], [13], underwater sensing [14]–[16], and driver assistance systems [17], [18]. Despite the diversity of applications, change detection researchers employ many common processing steps and core algorithms. The goal of this paper is to present a systematic survey of these steps and algorithms. Previous surveys of change detection were written by Singh in 1989 [19] and Coppin and Bauer in 1996 [20]. These articles discussed only remote-sensing methodologies. Here, we focus on more recent work from the broader (English-speaking) image analysis community that reflects the richer set of tools that have since been brought to bear on the topic.

The core problem discussed in this paper is as follows. We are given a set of images of the same scene taken at several different

times. The goal is to identify the set of pixels that are “significantly different” between the last image of the sequence and the previous images; these pixels comprise the *change mask*. The change mask may result from a combination of underlying factors, including appearance or disappearance of objects, motion of objects relative to the background, or shape changes of objects. In addition, stationary objects can undergo changes in brightness or color. A key issue is that the change mask should *not* contain “unimportant” or “nuisance” forms of change, such as those induced by camera motion, sensor noise, illumination variation, nonuniform attenuation, or atmospheric absorption. The notions of “significantly different” and “unimportant” vary by application, which sometimes makes it difficult to directly compare algorithms.

Estimating the change mask is often a first step toward the more ambitious goal of *change understanding*: segmenting and classifying changes by semantic type, which usually requires tools tailored to a particular application. The present survey emphasizes the detection problem, which is largely application independent. We do not discuss algorithms that are specialized to application-specific object classes, such as parts of human bodies in surveillance imagery [3] or buildings in overhead imagery [6], [21]. Furthermore, our interest here is only in methods that detect changes between raw images, as opposed to those that detect changes between hand-labeled region classes. In remote sensing, the latter approach is called “post-classification comparison” or “delta classification”.<sup>1</sup> Finally, we do not address two other problems from different fields that are sometimes called “change detection”: first, the estimation theory problem of determining the point at which signal samples are drawn from a new probability distribution (see, e.g., [24]), and second, the video processing problem of determining the frame at which an image sequence switches between scenes (see, e.g., [25], [26]).

We begin in Section II by formally defining the change detection problem and illustrating different mechanisms that can produce apparent image change. The remainder of the survey is organized by the main computational steps involved in change detection. Section III describes common types of geometric and radiometric image preprocessing operations. Section IV describes the simplest class of algorithms for making the change decision based on image differencing. The subsequent Sections V–VII

Manuscript received November 25, 2003; revised August 3, 2004. This research was supported in part by the National Science Foundation Center for Subsurface Sensing and Imaging Systems (CenSSIS) under the Engineering Research Center’s program of the National Science Foundation (Award Number EEC-9986821) and in part by Rensselaer Polytechnic Institute. The associate editor coordinating the review of this manuscript and approving it for publication was Dr. Joachim M. Buhmann.

The authors are with the Department of Electrical, Computer, and Systems Engineering, Rensselaer Polytechnic Institute, Troy, NY, 12180 USA (e-mail: rjradke@ecse.rpi.edu; andras@rpi.edu; alkofo@rpi.edu; roysam@ecse.rpi.edu).

Digital Object Identifier 10.1109/TIP.2004.838698

<sup>1</sup>Such methods were shown to have generally poor performance [19], [20]. We note that Deer and Eklund [22] described an improved variant where the class labels were allowed to be fuzzy, and that Bruzzone and Serpico [23] described a supervised learning algorithm for estimating the prior, transition, and posterior class probabilities using labeled training data and an adaptive neural network.

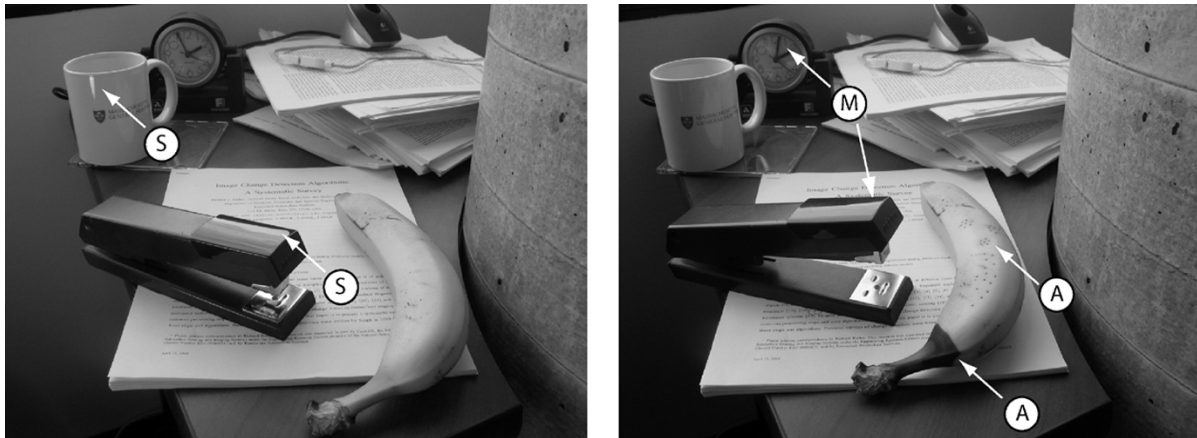


Fig. 1. Apparent image changes have many underlying causes. This simple example includes changes due to different camera- and light-source positions, as well as changes due to nonrigid object motion (labeled “M”), specular reflections (labeled “S”), and object appearance variations (labeled “A”). Deciding and detecting which changes are considered significant and which are considered unimportant are difficult problems and vary by application.

survey more sophisticated approaches to making the change decision, including significance and hypothesis tests, predictive models, and the shading model. With a few exceptions, the default assumption in these sections is that only two images are available to make the change decision. However, in some scenarios, a sequence of many images is available, and in Section VIII, we discuss background modeling techniques that exploit this information for change detection. Section IX focuses on steps taken during or following change mask estimation that attempt to enforce spatial or temporal smoothness in the masks. Section X discusses principles and methods for evaluating and comparing the performance of change detection algorithms. We conclude in the final section by mentioning recent trends and directions for future work.

## II. MOTIVATION AND PROBLEM STATEMENT

To make the change detection problem more precise, let  $\{I_1, I_2, \dots, I_M\}$  be an image sequence in which each image maps a pixel coordinate  $\mathbf{x} \in \mathbb{R}^l$  to an intensity or color  $I(\mathbf{x}) \in \mathbb{R}^k$ . Typically,  $k = 1$  (e.g., gray-scale images) or  $k = 3$  (e.g., RGB color images), but other values are possible. For instance, multispectral images have values of  $k$  in the tens, while hyperspectral images have values in the hundreds. Typically,  $l = 2$  (e.g., satellite or surveillance imagery) or  $l = 3$  (e.g., volumetric medical or biological microscopy data). Much of the work surveyed assumes either that  $M = 2$ , as is the case where satellite views of a region are acquired several months apart, or that  $M$  is very large, as is the case when images are captured several times a second from a surveillance camera.

A basic change detection algorithm takes the image sequence as input and generates a binary image  $B : \mathbb{R}^l \rightarrow [0, 1]$  called a *change mask* that identifies changed regions in the last image according to the following generic rule:

$$B(\mathbf{x}) = \begin{cases} 1, & \text{if there is a significant change at pixel } \mathbf{x} \text{ of } I_M \\ 0, & \text{otherwise.} \end{cases}$$

Fig. 1 is a toy example that illustrates the complexity of a real change detection problem, containing two images of a stapler and a banana taken several minutes apart. The apparent intensity

change at each pixel is due to a variety of factors. The camera has moved slightly. The direct and ambient light sources have changed position and intensity. The objects have been moved independently of the camera. In addition, the stapler arm has moved independently of the base, and the banana has deformed nonrigidly. Specular reflections on the stapler have changed, and the banana has changed color over time.

Fig. 2 is a real biomedical example showing a pair of images of the human retina taken six months apart. The images need to be registered, and contain several local illumination artifacts at the borders of the images. The gray spots in the right image indicate atrophy of the retinal tissue. Changes involving the vasculature are also present, especially a vessel marked “V” that has been cut off from the blood supply.

In both cases, it is difficult to say what the gold-standard or ground-truth change mask should be; this concept is generally application-specific. For example, in video surveillance, it is generally undesirable to detect the “background” revealed as a consequence of camera and object motion as change, whereas in remote sensing, this change might be considered significant (e.g., different terrain is revealed as a forest recedes). In the survey below, we try to be concrete about what the authors consider to be significant change and how they go about detecting it.

The change detection problem is intimately involved with several other classical computer vision problems that have a substantial literature of their own, including image registration, optical flow, object segmentation, tracking, and background modeling. Where appropriate, we have provided recent references where the reader can learn more about the state of the art in these fields.

## III. PREPROCESSING METHODS

The goal of a change detection algorithm is to detect “significant” changes while rejecting “unimportant” ones. Sophisticated methods for making this distinction require detailed modeling of all the expected types of changes (important and unimportant) for a given application and integration of these models into an effective algorithm. The following subsections describe

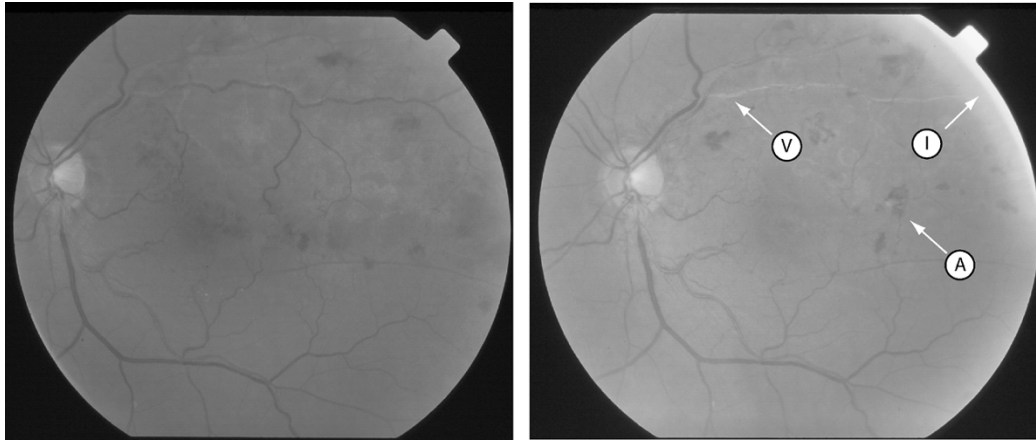


Fig. 2. Biomedical change detection example involving a pair of images of the same human retina taken six months apart. This example contains several changes involving the vasculature (labeled “V”) and numerous other important changes in the surrounding retinal tissue (labeled “A”). It also contains many illumination artifacts at the periphery (labeled “I”). It is of interest to detect the significant changes while rejecting registration and illumination artifacts.

preprocessing steps used to suppress or filter out common types of “unimportant” changes before making the change detection decision. These steps generally involve geometric and radiometric (i.e., intensity) adjustments.

#### A. Geometric Adjustments

Apparent intensity changes at a pixel resulting from camera motion alone are virtually never desired to be detected as real changes. Hence, a necessary preprocessing step for all change detection algorithms is accurate *image registration*, the alignment of several images into the same coordinate frame.

When the scenes of interest are mostly rigid in nature and the camera motion is small, registration can often be performed using low-dimensional spatial transformations such as similarity, affine, or projective transformations. This estimation problem has been well studied, and several excellent surveys [27]–[30], and software implementations (e.g., the Insight toolkit [31]) are available, so we do not detail registration algorithms here. Rather, we note some of the issues that are important from a change detection standpoint.

Choosing an appropriate spatial transformation is critical for good change detection. An excellent example is registration of curved human retinal images [32], for which an affine transformation is inadequate but a 12-parameter quadratic model suffices. Several modern registration algorithms are capable of switching automatically to higher order transformations after being initialized with a low-order similarity transformation [33]. In some scenarios (e.g., when the cameras that produced the images have widely spaced optical centers, or when the scene consists of deformable/articulated objects), a nonglobal transformation may need to be estimated to determine corresponding points between two images, e.g., via optical flow [34], tracking [35], object recognition and pose estimation [36], [37], or structure-from-motion [38], [39] algorithms.<sup>2</sup>

Another practical issue regarding registration is the selection of feature-based, intensity-based, or hybrid registration algorithms. In particular, when feature-based algorithms are used,

the accuracy of the features themselves must be considered in addition to the accuracy of the registration algorithm. One must consider the possibility of localized registration errors that can result in false change detection, even when average/global error measures appear to be modest.

Several researchers have studied the effects of registration errors on change detection, especially in the context of remote sensing [40], [41]. Dai and Khorram [42] progressively translated one multispectral image against itself and analyzed the sensitivity of a difference-based change detection algorithm (see Section IV). They concluded that highly accurate registration was required to obtain good change detection results (e.g., one-fifth-pixel registration accuracy to obtain change detection error of less than 10%). Bruzzone and Cossu [43] did a similar experiment on two-channel images and obtained a nonparametric density estimate of registration noise over the space of change vectors. They then developed a change detection strategy that incorporated this *a priori* probability that change at a pixel was due to registration noise.

#### B. Radiometric/Intensity Adjustments

In several change detection scenarios (e.g., surveillance), intensity variations in images caused by changes in the strength or position of light sources in the scene are considered unimportant. Even in cases where there are no actual light sources involved, there may be physical effects with similar consequences on the image (e.g., calibration errors and variations in imaging system components in magnetic resonance and computed tomography imagery). In this section, we describe several techniques that attempt to precompensate for illumination variations between images. Alternately, some change detection algorithms are designed to cope with illumination variation without explicit preprocessing (see Section VII).

1) *Intensity Normalization*: Some of the earliest attempts at illumination-invariant change detection used intensity normalization [44], [45], and it is still used [42]. The pixel intensity values in one image are normalized to have the same mean and variance as those in another, i.e.

$$\tilde{I}_2(\mathbf{x}) = \frac{\sigma_1}{\sigma_2} \{I_2(\mathbf{x}) - \mu_2\} + \mu_1 \quad (1)$$

<sup>2</sup>We note that these nonglobal processes are ordinarily not referred to as “registration” in the literature.

where  $\tilde{I}_2$  is the normalized second image and  $\mu_i, \sigma_i$  are the mean and standard deviation of the intensity values of  $I_i$ , respectively. Alternatively, both images can be normalized to have zero mean and unit variance. This allows the use of decision thresholds that are independent of the original intensity values of the images.

Instead of applying the normalization (1) to each pixel using the global statistics  $\mu_i, \sigma_i$ , the images can be divided into corresponding disjoint blocks, and the normalization independently performed using the local statistics of each block. This can achieve better local performance at the expense of introducing blocking artifacts.

2) *Homomorphic Filtering*: For images of scenes containing Lambertian surfaces, the observed image intensity at a pixel  $\mathbf{x}$  can be modeled as the product of two components: the illumination  $I_l(\mathbf{x})$  from the light source(s) in the scene and the reflectance  $I_o(\mathbf{x})$  of the object surface to which  $\mathbf{x}$  belongs

$$I(\mathbf{x}) = I_l(\mathbf{x})I_o(\mathbf{x}). \quad (2)$$

This is called the *shading model* [46]. Only the reflectance component  $I_o(\mathbf{x})$  contains information about the objects in the scene. A type of illumination-invariant change detection can, hence, be performed by first filtering out the illumination component from the image. If the illumination due to the light sources  $I_l(\mathbf{x})$  has lower spatial frequency content than the reflectance component  $I_o(\mathbf{x})$ , a *homomorphic filter* can be used to separate the two components of the intensity signal. That is, logarithms are taken on both sides of (2) to obtain

$$\ln I(\mathbf{x}) = \ln I_l(\mathbf{x}) + \ln I_o(\mathbf{x}).$$

Since the lower frequency component  $\ln I_l(\mathbf{x})$  is now additive, it can be separated using a high-pass filter. The reflectance component can thus be estimated as

$$\tilde{I}_o(\mathbf{x}) = \exp\{F(\ln I(\mathbf{x}))\}$$

where  $F(\cdot)$  is a high-pass filter. The reflectance component can be provided as input to the decision rule step of a change detection process (see, e.g., [47], [48]).

3) *Illumination Modeling*: Modeling and compensating for local radiometric variation that deviates from the Lambertian assumption is necessary in several applications (e.g., underwater imagery [49]). For example, the illumination component can be modeled as a piecewise polynomial function. Negahdaripour [50] proposed a generic linear model for radiometric variation between images of the same scene

$$I_2(x, y) = M(x, y)I_1(x, y) + A(x, y)$$

where  $M(x, y)$  and  $A(x, y)$  are piecewise smooth functions with discontinuities near region boundaries. Hager and Belhumeur [51] used principal component analysis (PCA) to extract a set of basis images  $B_k(x, y)$  that represent the views of a scene under all possible lighting conditions, so that after registration

$$I_2(x, y) = I_1(x, y) + \sum_{k=1}^K \alpha_k B_k(x, y).$$

In our experience, these sophisticated models of illumination compensation are not commonly used in the context of change detection. However, Bromiley *et al.* [52] proposed several ways that the scattergram, or joint histogram of image intensities, could be used to estimate and remove a global nonparametric illumination model from an image pair prior to simple differencing. The idea is related to mutual information measures used for image registration [53].

4) *Linear Transformations of Intensity*: In the remote-sensing community, it is common to transform a multispectral image into a different intensity space before proceeding to change detection. For example, Jensen [54] and Niemeyer *et al.* [55] discussed applying PCA to the set of all bands from two multispectral images. The principal component images corresponding to large eigenvalues are assumed to reflect the unchanged part of the images, and those corresponding to smaller eigenvalues to changed parts of the images. The difficulty with this approach is determining which of the principal components represent change without visual inspection. Alternately, one can apply PCA to difference images as in Gong [56], in which case, the first one or two principal component images are assumed to represent changed regions.

Another linear transformation for change detection in remote-sensing applications using Landsat data is the Kauth–Thomas, or “Tasseled Cap,” transform [57]. The transformed intensity axes are linear combinations of the original Landsat bands and have semantic descriptions including “soil brightness,” “green vegetation,” and “yellow stuff.” Collins and Woodcock [5] compared different linear transformations of multispectral intensities for mapping forest changes using Landsat data. Morissette and Khorram [58] discussed how both an optimal combination of multispectral bands and a corresponding decision threshold to discriminate change could be estimated using a neural network from training data regions labeled as change/no change.

In surveillance applications, Elgammal *et al.* [59] observed that the coordinates  $(G/(R + G + B), B/(R + G + B), R + G + B)$  are more effective than RGB coordinates for suppressing unwanted changes due to shadows of objects.

5) *Sudden Changes in Illumination*: Xie *et al.* [60] observed that, under the Phong shading model with slowly spatially varying illumination, the sign of the difference between corresponding pixel measurements is invariant to sudden changes in illumination. They used this result to create a change detection algorithm that is able to discriminate between “uninteresting” changes caused by a sudden change in illumination (e.g., turning on a light switch) and “interesting” changes caused by object motion (see also the background modeling techniques discussed in Section VIII).

Watanabe *et al.* [21] discussed an interesting radiometric preprocessing step specifically for change detection applied to overhead imagery of buildings. Using the known position of the sun and a method for fitting building models to images, they were able to remove strong shadows of buildings due to direct light from the sun, prior to applying a change detection algorithm.

6) *Speckle Noise*: Speckle is an important type of noise-like artifact found in coherent imagery, such as synthetic aperture radar and ultrasound. There is a sizable body of research

(too large to summarize here) on modeling and suppression of speckle (for example, see [61]–[63] and the survey by Touzi [64]). Common approaches to suppressing false changes due to speckle include frame averaging (assuming speckle is uncorrelated between successive images), local spatial averaging (albeit at the expense of spatial resolution), thresholding, and statistical model-based and/or multiscale filtering.

#### IV. SIMPLE DIFFERENCING

Early change detection methods were based on the signed difference image  $D(\mathbf{x}) = I_2(\mathbf{x}) - I_1(\mathbf{x})$ , and such approaches are still widespread. The most obvious algorithm is to simply threshold the difference image. That is, the change mask  $B(\mathbf{x})$  is generated according to the following decision rule:

$$B(\mathbf{x}) = \begin{cases} 1, & \text{if } |D(\mathbf{x})| > \tau \\ 0, & \text{otherwise.} \end{cases}$$

We denote this algorithm as “simple differencing.” Often, the threshold  $\tau$  is chosen empirically. Rosin [65], [66] surveyed and reported experiments on many different criteria for choosing  $\tau$ . Smits and Annoni [67] discussed how the threshold can be chosen to achieve application-specific requirements for false alarms and misses (i.e., the choice of point on a receiver-operating-characteristics curve [68]; see Section X).

There are several methods that are closely related to simple differencing. For example, in *change vector analysis* (CVA) [4], [69]–[71], often used for multispectral images, a feature vector is generated for each pixel in the image, considering several spectral channels. The modulus of the difference between the two feature vectors at each pixel gives the values of the “difference image.”<sup>3</sup> *Image ratioing* is another related technique that uses the ratio, instead of the difference, between the pixel intensities of the two images [19]. DiStefano *et al.* [72] performed simple differencing on subsampled gradient images. Tests that have similar functional forms but are more well defended from a theoretical perspective are discussed further in Sections VI and VII below.

However the threshold is chosen, simple differencing with a global threshold is unlikely to outperform the more advanced algorithms discussed below in any real-world application. This technique is sensitive to noise and variations in illumination and does not consider local consistency properties of the change mask.

#### V. SIGNIFICANCE AND HYPOTHESIS TESTS

The decision rule in many change detection algorithms is cast as a statistical hypothesis test. The decision as to whether or not a change has occurred at a given pixel  $\mathbf{x}$  corresponds to choosing one of two competing hypotheses: the *null hypothesis*  $\mathcal{H}_0$  or the *alternative hypothesis*  $\mathcal{H}_1$ , corresponding to *no-change* and *change* decisions, respectively.

The image pair  $(I_1(\mathbf{x}), I_2(\mathbf{x}))$  is viewed as a random vector. Knowledge of the conditional joint probability density functions (pdfs)  $p(I_1(\mathbf{x}), I_2(\mathbf{x})|\mathcal{H}_0)$ , and  $p(I_1(\mathbf{x}), I_2(\mathbf{x})|\mathcal{H}_1)$  allows us to

<sup>3</sup>In some cases, the direction of this vector can also be used to discriminate between different types of changes [43].

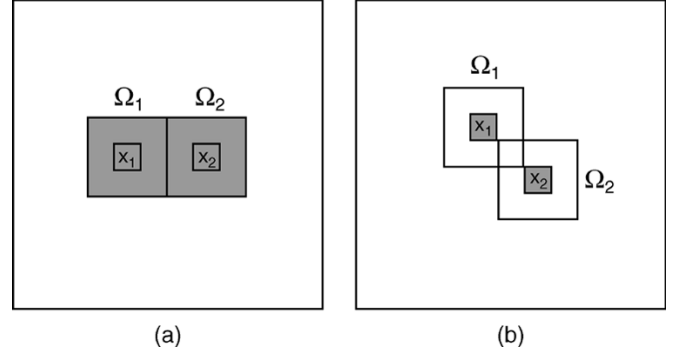


Fig. 3. Two block-based approaches. (a) The decision is applied to the entire block of pixels  $\Omega_{\mathbf{x}}$ . (b) The decision is applied only to the center pixel  $\mathbf{x}$ . In case (a), the blocks  $\Omega_{\mathbf{x}}$  do not overlap, but in case (b), they do. Approach (b) is generally preferred.

choose the hypothesis that best describes the intensity change at  $\mathbf{x}$  using the classical framework of hypothesis testing [68], [73].

Since interesting changes are often associated with localized groups of pixels, it is common for the change decision at a given pixel  $\mathbf{x}$  to be based on a small block of pixels in the neighborhood of  $\mathbf{x}$  in each of the two images (such approaches are also called “geo-pixel” methods). Alternately, decisions can be made independently at each pixel and then processed to enforce smooth regions in the change mask (see Section IX).

We denote a block of pixels centered at  $\mathbf{x}$  by  $\Omega_{\mathbf{x}}$ . The pixel values in the block are denoted

$$\hat{I}(\mathbf{x}) = \{I(\mathbf{y}) \mid \mathbf{y} \in \Omega_{\mathbf{x}}\}.$$

Note that  $\hat{I}(\mathbf{x})$  is an ordered set to ensure that corresponding pixels in the image pair are matched correctly. We assume that the block contains  $N$  pixels. There are two methods for dealing with blocks, as illustrated in Fig. 3. One option is to apply the decision reached at  $\mathbf{x}$  to all the pixels in the block  $\Omega_{\mathbf{x}}$  [Fig. 3(a)], in which case the blocks do not overlap, the change mask is coarse, and block artifacts are likely. The other option is to apply the decision only to pixel  $\mathbf{x}$  [Fig. 3(b)], in which case the blocks can overlap and there are fewer artifacts; however, this option is computationally more expensive.

##### A. Significance Tests

Characterizing the null hypothesis  $\mathcal{H}_0$  is usually straightforward, since in the absence of any change, the difference between image intensities can be assumed to be due to noise alone. A *significance test* on the difference image can be performed to assess how well the null hypothesis describes the observations, and this hypothesis is correspondingly accepted or rejected. The test is carried out as below

$$S(\mathbf{x}) = p(D(\mathbf{x})) \mid \mathcal{H}_0 \underset{\mathcal{H}_1}{\overset{\mathcal{H}_0}{\geq}} \tau.$$

The threshold  $\tau$  can be computed to produce a desired false alarm rate  $\alpha$ .

Aach *et al.* [74], [75] modeled the observation  $D(\mathbf{x})$  under the null hypothesis as a Gaussian random variable with zero mean and variance  $\sigma_0^2$ . The unknown parameter  $\sigma_0^2$  can be estimated offline from the imaging system or recursively from unchanged

regions in an image sequence [76]. In the Gaussian case, this results in the conditional pdf

$$p(D(\mathbf{x}) | \mathcal{H}_0) = \frac{1}{\sqrt{2\pi\sigma_0^2}} \exp \left\{ -\frac{D^2(\mathbf{x})}{2\sigma_0^2} \right\}. \quad (3)$$

They also considered a Laplacian noise model that is similar.

The extension to a block-based formulation is straightforward. Though there are obvious statistical dependencies within a block, the observations for each pixel in a block are typically assumed to be independent and identically distributed (iid). For example, the block-based version of the significance test (3) uses the test statistic

$$\begin{aligned} p(\hat{D}(\mathbf{x}) | \mathcal{H}_0) &= \left( \frac{1}{\sqrt{2\pi\sigma_0^2}} \right)^N \exp \left\{ -\frac{\sum_{\mathbf{y} \in \Omega_{\mathbf{x}}} D^2(\mathbf{y})}{2\sigma_0^2} \right\} \\ &= \left( \frac{1}{\sqrt{2\pi\sigma_0^2}} \right)^N \exp \left\{ -\frac{G(\mathbf{x})}{2} \right\}. \end{aligned}$$

Here,  $G(\mathbf{x}) = \left( \sum_{\mathbf{y} \in \Omega_{\mathbf{x}}} D^2(\mathbf{y}) \right) / \sigma_0^2$ , which has a  $\chi^2$  pdf with  $N$  degrees of freedom. Tables for the  $\chi^2$  distribution can be used to compute the decision threshold for a desired false alarm rate. A similar computation can be performed when each observation is modeled as an independent Laplacian random variable.

### B. Likelihood Ratio Tests

Characterizing the alternative (change) hypothesis  $\mathcal{H}_1$  is more challenging, since the observations consist of change components that are not known *a priori* or cannot easily be described by parametric distributions. When both conditional pdfs are known, a *likelihood ratio* can be formed as

$$L(\mathbf{x}) = \frac{p(D(\mathbf{x}) | \mathcal{H}_1)}{p(D(\mathbf{x}) | \mathcal{H}_0)}.$$

This ratio is compared to a threshold  $\tau$  defined as

$$\tau = \frac{P(\mathcal{H}_0)(C_{10} - C_{00})}{P(\mathcal{H}_1)(C_{01} - C_{11})}$$

where  $P(\mathcal{H}_i)$  is the *a priori* probability of hypothesis  $\mathcal{H}_i$ , and  $C_{ij}$  is the cost associated with making a decision in favor of hypothesis  $\mathcal{H}_i$  when  $\mathcal{H}_j$  is true. In particular,  $C_{10}$  is the cost associated with “false alarms” and  $C_{01}$  is the cost associated with “misses.” If the likelihood ratio at  $\mathbf{x}$  exceeds  $\tau$ , a decision is made in favor of hypothesis  $\mathcal{H}_1$ ; otherwise, a decision is made in favor of hypothesis  $\mathcal{H}_0$ . This procedure yields the minimum *Bayes risk* by choosing the hypothesis that has the maximum *a posteriori* probability of having occurred given the observations ( $I_1(\mathbf{x}), I_2(\mathbf{x})$ ).

Aach *et al.* [74], [75] characterized both hypotheses by modeling the observations comprising  $\hat{D}(\mathbf{x})$  under  $\mathcal{H}_i$  as iid zero-mean Gaussian random variables with variance  $\sigma_i^2$ . In this case, the block-based likelihood ratio is given by

$$\frac{p(\hat{D}(\mathbf{x}) | \mathcal{H}_1)}{p(\hat{D}(\mathbf{x}) | \mathcal{H}_0)} = \frac{\sigma_0^N}{\sigma_1^N} \exp \left\{ -\sum_{\mathbf{y} \in \Omega_{\mathbf{x}}} D^2(\mathbf{y}) \left( \frac{1}{2\sigma_1^2} - \frac{1}{2\sigma_0^2} \right) \right\}.$$

The parameters  $\sigma_0^2$  and  $\sigma_1^2$  were estimated from unchanged [i.e., very small  $D(\mathbf{x})$ ] and changed [i.e., very large  $D(\mathbf{x})$ ] regions of the difference image, respectively. As before, they also considered a similar Laplacian noise model. Rignot and van Zyl [77] described hypothesis tests on the difference and ratio images from SAR data assuming the true and observed intensities were related by a gamma distribution.

Bruzzzone and Prieto [69] noted that while the variances estimated as above may serve as good initial guesses, using them in a decision rule may result in a false alarm rate different from the desired value. They proposed an automatic change detection technique that estimates the parameters of the mixture distribution  $p(D)$  consisting of all pixels in the difference image. The mixture distribution  $p(D)$  can be written as

$$p(D(\mathbf{x})) = p(D(\mathbf{x}) | \mathcal{H}_0)P(\mathcal{H}_0) + p(D(\mathbf{x}) | \mathcal{H}_1)P(\mathcal{H}_1).$$

The means and variances of the class conditional distributions  $p(D(\mathbf{x}) | \mathcal{H}_i)$  are estimated using an expectation-maximization (EM) algorithm [78] initialized in a similar way to the algorithm of Aach *et al.* In [4], Bruzzzone and Prieto proposed a more general algorithm where the difference image is initially modeled as a mixture of two nonparametric distributions obtained by the reduced Parzen estimate procedure [79]. These nonparametric estimates are iteratively improved using an EM algorithm. We note that these methods can be viewed as a precursor to the more sophisticated background modeling approaches described in Section VIII.

### C. Probabilistic Mixture Models

This category is best illustrated by Black *et al.* [80], who described an innovative approach to estimating changes. Instead of classifying the pixels as change/no change as above, or as object/background as in Section VIII, they are softly classified into mixture components corresponding to different generative models of change. These models included 1) parametric object or camera motion, 2) illumination phenomena, 3) specular reflections, and 4) “iconic/pictorial changes” in objects, such as an eye blinking or a nonrigid object deforming (using a generative model learned from training data). A fifth outlier class collects pixels poorly explained by any of the four generative models. The algorithm operates on the optical flow field between an image pair and uses the EM algorithm to perform a soft assignment of each vector in the flow field to the various classes. The approach is notable in that image registration and illumination variation parameters are estimated in-line with the changes, instead of beforehand. This approach is quite powerful, capturing multiple object motions, shadows, specularities, and deformable models in a single framework.

### D. Minimum Description Length

To conclude this section, we note that Leclerc *et al.* [81] proposed a change detection algorithm based on a concept called “self-consistency” between viewpoints of a scene. The algorithm involves both raw images and three-dimensional (3-D) terrain models, so it is not directly comparable to the methods

surveyed above; the main goal of the work is to provide a framework for measuring the performance of stereo algorithms. However, a notable feature of this approach is its use of the minimum description length (MDL) model selection principle [82] to classify unchanged and changed regions, as opposed to the Bayesian approaches discussed earlier. The MDL principle selects the hypothesis  $\mathcal{H}_i$  that more concisely describes (i.e., using a smaller number of bits) the observed pair of images. We believe MDL-based model selection approaches have great potential for “standard” image change detection problems and are worthy of further study.

## VI. PREDICTIVE MODELS

More sophisticated change detection algorithms result from exploiting the close relationships between nearby pixels both in space and time (when an image sequence is available).

### A. Spatial Models

A classical approach to change detection is to fit the intensity values of each block to a polynomial function of the pixel coordinates  $\mathbf{x}$ . In two dimensions, this corresponds to

$$\hat{I}_k(x, y) = \sum_{i=0}^p \sum_{j=0}^{p-i} \beta_{ij}^k x^i y^j \quad (4)$$

where  $p$  is the order of the polynomial model. Hsu *et al.* [83] discussed generalized likelihood ratio tests using a constant, linear, or quadratic model for image blocks. The null hypothesis in the test is that corresponding blocks in the two images are best fit by the same polynomial coefficients  $\beta_{ij}^0$ , whereas the alternative hypothesis is that the corresponding blocks are best fit by different polynomial coefficients  $(\beta_{ij}^1, \beta_{ij}^2)$ . In each case, the various model parameters  $\beta_{ij}^k$  are obtained by a least-squares fit to the intensity values in one or both corresponding image blocks. The likelihood ratio is obtained based on derivations by Yakimovsky [84] and is expressed as

$$F(\mathbf{x}) = \frac{\sigma_0^{2N}}{\sigma_1^N \sigma_2^N}$$

where  $N$  is the number of pixels in the block,  $\sigma_1^2$  is the variance of the residuals from the polynomial fit to the block in  $I_1$ ,  $\sigma_2^2$  is the variance of the residuals from the polynomial fit to the block in  $I_2$ , and  $\sigma_0^2$  is the variance of the residuals from the polynomial fit to both blocks simultaneously. The threshold in the generalized likelihood ratio test can be obtained using the  $t$ -test (for a constant model) or the  $F$ -test (for linear and quadratic models). Hsu *et al.* used these three models to detect changes between a pair of surveillance images and concluded that the quadratic model outperformed the other two models, yielding similar change detection results but with higher confidence.

Skifstad and Jain [85] suggested an extension of Hsu’s intensity modeling technique to make it illumination-invariant.

The authors suggested a test statistic that involved spatial partial derivatives of Hsu’s quadratic model, given by

$$T(\mathbf{x}) = \sum_{\mathbf{y} \in \Omega_{\mathbf{x}}} \left( \frac{\partial \hat{I}_1}{\partial x}(\mathbf{y}) - \frac{\partial \hat{I}_2}{\partial x}(\mathbf{y}) + \frac{\partial \hat{I}_1}{\partial y}(\mathbf{y}) - \frac{\partial \hat{I}_2}{\partial y}(\mathbf{y}) \right). \quad (5)$$

Here, the intensity values  $\hat{I}_j(\mathbf{x})$  are modeled as quadratic functions of the pixel coordinates [i.e., (4) with  $p = 2$ ]. The test statistic is compared to an empirical threshold to classify pixels as changed or unchanged. Since the test statistic only involves partial derivatives, it is independent of linear variations in intensity. As with homomorphic filtering, the implicit assumption is that illumination variations occur at lower spatial frequencies than changes in the objects. It is also assumed that true changes in image objects will be reflected by different coefficients in the quadratic terms that are preserved by the derivative.

### B. Temporal Models

When the change detection problem occurs in the context of an image sequence, it is natural to exploit the temporal consistency of pixels in the same location at different times.

Many authors have modeled pixel intensities over time as an autoregressive (AR) process. An early reference is Elfishawy *et al.* [86]. More recently, Jain and Chau [87] assumed each pixel was identically and independently distributed according to the same (time varying) Gaussian distribution related to the past by the same (time varying) AR(1) coefficient. Under these assumptions, they derived maximum likelihood estimates of the mean, variance, and correlation coefficient at each point in time, and used these in likelihood ratio tests where the null (no-change) hypothesis is that the image intensities are dependent, and the alternate (change) hypothesis is that the image intensities are independent (this is similar to Yakimovsky’s hypothesis test above).

Similarly, Toyama *et al.* [88] described an algorithm called Wallflower that used a Wiener filter to predict a pixel’s current value from a linear combination of its  $k$  previous values. Pixels whose prediction error is several times worse than the expected error are classified as changed pixels. The predictive coefficients are adaptively updated at each frame. This can also be thought of as a background estimation algorithm (see Section VIII). The Wallflower algorithm also tries to correctly classify the interiors of homogeneously colored, moving objects by determining the histogram of connected components of change pixels and adding pixels to the change mask based on distance and color similarity. Morissette and Khorram’s work [58], discussed in Section III-B, can be viewed as a supervised method to determine an optimal linear predictor.

Carlotto [89] claimed that linear models perform poorly and suggested a nonlinear dependence to model the relationship between two images in a sequence  $I_i(\mathbf{x})$  and  $I_j(\mathbf{x})$  under the no-change hypothesis. The optimal nonlinear function is simply  $f_{ij}$ , the conditional expected value of the intensity  $I_i(\mathbf{x})$  given  $I_j(\mathbf{x})$ . For an  $N$ -image sequence, there are  $N(N-1)/2$  total residual error images

$$\epsilon_{ij}(x, y) = [I_i(x, y) - f_{ij}(I_j(\mathbf{x}))] - [I_j(x, y) - f_{ji}(I_i(\mathbf{x}))].$$



These images are then thresholded to produce binary change masks. Carlotto went on to detect specific temporal patterns of change by matching the string of  $N$  binary change decisions at a pixel with a desired input pattern.

Clifton [90] used an adaptive neural network to identify small-scale changes from a sequence of overhead multispectral images. This can be viewed as an unsupervised method for learning the parameters of a nonlinear predictor. Pixels for which the predictor performs poorly are classified as changed. The goal is to distinguish “unusual” changes from “expected” changes, but this terminology is somewhat vague, and does not seem to correspond directly to the notions of “foreground” and “background” in Section VIII.

## VII. SHADING MODEL

Several change detection techniques are based on the shading model for the intensity at a pixel as described in Section III-B to produce an algorithm that is said to be illumination-invariant. Such algorithms generally compare the ratio of image intensities

$$R(\mathbf{x}) = \frac{I_2(\mathbf{x})}{I_1(\mathbf{x})}$$

to a threshold determined empirically. We now show the rationale for this approach.

Assuming shading models for the intensities  $I_1(\mathbf{x})$  and  $I_2(\mathbf{x})$ , we can write  $I_1(\mathbf{x}) = I_{l1}(\mathbf{x})I_{o1}(\mathbf{x})$  and  $I_2(\mathbf{x}) = I_{l2}(\mathbf{x})I_{o2}(\mathbf{x})$ , which implies

$$\frac{I_2(\mathbf{x})}{I_1(\mathbf{x})} = \frac{I_{l2}(\mathbf{x})I_{o2}(\mathbf{x})}{I_{l1}(\mathbf{x})I_{o1}(\mathbf{x})}. \quad (6)$$

Since the reflectance component  $I_{oi}(\mathbf{x})$  depends only on the intrinsic properties of the object surface imaged at  $\mathbf{x}$ ,  $I_{o1}(\mathbf{x}) = I_{o2}(\mathbf{x})$  in the absence of a change. This observation simplifies (6) to

$$\frac{I_2(\mathbf{x})}{I_1(\mathbf{x})} = \frac{I_{l2}(\mathbf{x})}{I_{l1}(\mathbf{x})}.$$

Hence, if the illuminations  $I_{l1}$  and  $I_{l2}$  in each image are approximated as constant within a block  $\Omega_{\mathbf{x}}$ , the ratio of intensities  $I_2(\mathbf{x})/I_1(\mathbf{x})$  remains constant under the null hypothesis  $\mathcal{H}_0$ . This justifies a null hypothesis that assumes linear dependence between vectors of corresponding pixel intensities, giving rise to the test statistic  $R(\mathbf{x})$ .

Skifstad and Jain [85] suggested the following method to assess the linear dependence between two blocks of pixel values  $\hat{I}_1(\mathbf{x})$  and  $\hat{I}_2(\mathbf{x})$ : construct

$$\eta(\mathbf{x}) = \frac{1}{N} \sum_{\mathbf{y} \in \Omega_{\mathbf{x}}} (R(\mathbf{x}) - \mu_{\mathbf{x}})^2 \quad (7)$$

where  $\mu_{\mathbf{x}}$  is given by

$$\mu_{\mathbf{x}} = \frac{1}{N} \sum_{\mathbf{y} \in \Omega_{\mathbf{x}}} R(\mathbf{x}).$$

When  $\eta(\mathbf{x})$  exceeds a threshold, a decision is made in favor of a change. The linear dependence detector (LDD) proposed by Durucan and Ebrahimi [91], [92] is closely related to the shading

model in both theory and implementation, mainly differing in the form of the linear dependence test (e.g., using determinants of Wronskian or Grammian matrices [93]).

Mester, Aach, and others [48], [94] criticized the test criterion (7) as *ad hoc*, and expressed the linear dependence model using a different hypothesis test. Under the null hypothesis  $\mathcal{H}_0$ , each image is assumed to be a function of a noise-free underlying image  $I(\mathbf{x})$ . The vectors of image intensities from corresponding  $N$ -pixel blocks centered at  $\mathbf{x}$  under the null hypothesis  $\mathcal{H}_0$  are expressed as

$$\begin{aligned} \hat{I}_1(\mathbf{x}) &= \hat{I}(\mathbf{x}) + \delta_1 \\ \hat{I}_2(\mathbf{x}) &= k\hat{I}(\mathbf{x}) + \delta_2. \end{aligned}$$

Here,  $k$  is an unknown scaling constant representing the illumination, and  $\delta_1, \delta_2$  are two realizations of a noise block in which each element is iid  $\mathcal{N}(0, \sigma_n^2)$ . The projection of  $\hat{I}_2(\mathbf{x})$  onto the subspace orthogonal to  $\hat{I}_1(\mathbf{x})$  is given by

$$\hat{O}(\mathbf{x}) = \hat{I}_2(\mathbf{x}) - \left( \frac{\hat{I}_1(\mathbf{x})^T \hat{I}_2(\mathbf{x})}{\|\hat{I}_1(\mathbf{x})\|^2} \right) \hat{I}_1(\mathbf{x}).$$

This is zero if, and only if,  $\hat{I}_1(\mathbf{x})$  and  $\hat{I}_2(\mathbf{x})$  are linearly dependent. The authors showed that in an appropriate basis, the joint pdf of the projection  $\hat{O}(\mathbf{x})$  under the null hypothesis  $\mathcal{H}_0$  is approximately a  $\chi^2$  distribution with  $N - 1$  degrees of freedom, and used this result both for significance and likelihood ratio tests.

Li and Leung [95] also proposed a change detection algorithm involving the shading model, using a weighted combination of the intensity difference and a texture difference measure involving the intensity ratio. The texture information is assumed to be less sensitive to illumination variations than the raw intensity difference. However, in homogeneous regions, the texture information becomes less valid and more weight is given to the intensity difference.

Liu *et al.* [96] suggested another change detection scheme that uses a significance test based on the shading model. The authors compared circular shift moments to detect changes instead of intensity ratios. These moments are designed to represent the reflectance component of the image intensity, regardless of illumination. The authors claimed that circular shift moments capture image object details better than the second-order statistics used in (7), and derived a set of iterative formulas to calculate the moments efficiently.

## VIII. BACKGROUND MODELING

In the context of surveillance applications, change detection is closely related to the well-studied problem of background modeling. The goal is to determine which pixels belong to the background, often prior to classifying the remaining foreground pixels (i.e., changed pixels) into different object classes.<sup>4</sup> Here, the change detection problem is qualitatively much different than in typical remote-sensing applications. A large amount of frame-rate video data is available, and the images between

<sup>4</sup>It is sometimes difficult to rigorously define what is meant by these terms. For example, a person may walk into a room and fall asleep in a chair. At what point does the motionless person transition from foreground to background?



which it is desired to detect changes are spaced apart by seconds rather than months. The entire image sequence is used as the basis for making decisions about change, as opposed to a single image pair. Furthermore, there is frequently an important semantic interpretation to the change that can be exploited (e.g., a person enters a room or a delivery truck drives down a street).

Several approaches to background modeling and subtraction were recently collected in a special issue of IEEE PAMI on video surveillance [1]. The reader is also referred to the results from the DARPA Visual Surveillance and Monitoring (VSAM) project at Carnegie-Mellon University [97] and elsewhere. Most background modeling approaches assume the camera is fixed, meaning the images are already registered (see the last paragraph in this section). Toyama *et al.* [88] gave a good overview of several background maintenance algorithms and provided a comparative example.

Many approaches fall into the mixture-of-Gaussians category: the probability of observing the intensity  $I_t(x, y)$  at location  $(x, y)$  and time  $t$  is the weighted sum of  $K$  Gaussian distributions

$$p_{I_t(x,y)}(C) = \sum_{i=1}^K w_t^i(x, y) \cdot (2\pi)^{k/2} |\Sigma_t^i(x, y)|^{-1/2} \times \exp\left(-\frac{1}{2}(C - \mu_t^i(x, y))^T \Sigma_t^i(x, y)^{-1} (C - \mu_t^i(x, y))\right).$$

At each point in time, the probability that a pixel's intensity is due to each of the mixtures is estimated, and the most likely mixture defines the pixel's class. The mean and covariance of each background pixel are usually initialized by observing several seconds of video of an empty scene. We briefly review several such techniques here.

Several researchers [98]–[100] have described adaptive background subtraction techniques in which a single Gaussian density is used to model the background. Foreground pixels are determined as those that lie some number of standard deviations from the mean background model and are clustered into objects. The mean and variance of the background are updated using simple adaptive filters to accommodate changes in lighting or objects that become part of the background. Collins *et al.* [97] augmented this approach with a second level of analysis to determine whether a pixel is due to a moving object, a stationary object, or an ambient illumination change. Gibbins *et al.* [101] had a similar goal of detecting suspicious changes in the background for video surveillance applications (e.g., a suitcase left in a bus station).

Wren *et al.* [3] proposed a method for tracking people and interpreting their behavior called Pfinder that included a background estimation module. This included not only a single Gaussian distribution for the background model at each pixel, but also a variable number of Gaussian distributions corresponding to different foreground object models. Pixels are classified as background or object by finding the model with the least Mahalanobis distance. Dynamic “blob” models for a person's head, hands, torso, etc. are then fit to the foreground pixels for each object, and the statistics for each object are updated. Hötter *et al.* [102] described a similar approach

for generic objects. Paragios and Tziritis [103] proposed an approach for finding moving objects in image sequences that further constrained the background/foreground map to be a Markov random field (see Section IX below).

Stauffer and Grimson [2] extended the multiple object model above to also allow the background model to be a mixture of several Gaussians. The idea is to correctly classify *dynamic* background pixels, such as the swaying branches of a tree or the ripples of water on a lake. Every pixel value is compared against the existing set of models at that location to find a match. The parameters for the matched model are updated based on a learning factor. If there is no match, the least-likely model is discarded and replaced by a new Gaussian with statistics initialized by the current pixel value. The models that account for some predefined fraction of the recent data are deemed “background” and the rest “foreground.” There are additional steps to cluster and classify foreground pixels into semantic objects and track the objects over time.

The Wallflower algorithm by Toyama *et al.* [88] described in Section VI also includes a frame-level background maintenance algorithm. The intent is to cope with situations where the intensities of most pixels change simultaneously, e.g., as the result of turning on a light. A “representative set” of background models is learned via  $k$ -means clustering during a training phase. The best background model is chosen on-line as the one that produces the lowest number of foreground pixels. Hidden Markov models can be used to further constrain the transitions between different models at each pixel [104], [105].

Haritaoglu *et al.* [106] described a background estimation algorithm as part of their  $W^4$  tracking system. Instead of modeling each pixel's intensity by a Gaussian, they analyzed a video segment of the empty background to determine the minimum ( $m$ ) and maximum ( $M$ ) intensity values, as well as the largest interframe difference ( $\delta$ ). If the observed pixel is more than  $\delta$  levels away from either  $m$  or  $M$ , it is considered foreground.

Instead of using Gaussian densities, Elgammal *et al.* [59] used a nonparametric kernel density estimate for the intensity of the background and each foreground object. That is

$$p_{I_t(x,y)}(C) = \frac{1}{N} \sum_{i=1}^N K_\sigma(C - I_{t-i}(x, y))$$

where  $K_\sigma$  is a kernel function with bandwidth  $\sigma$ . Pixel intensities that are unlikely based on the instantaneous density estimate are classified as foreground. An additional step that allows for small deviations in object position [(i.e., by comparing  $I_t(x, y)$  against the learned densities in a small neighborhood of  $(x, y)$ ] is used to suppress false alarms.

Ivanov *et al.* [107] described a method for background subtraction using multiple fixed cameras. A disparity map of the empty background is interactively built off line. On-line, foreground objects are detected as regions where pixels put into correspondence by the learned disparity map have inconsistent intensities. Latecki *et al.* [108] discussed a method for semantic change detection in video sequences (e.g., detecting whether an object enters the frame) using a histogram-based approach that does not identify which pixels in the image correspond to changes.

Ren *et al.* [109] extended a statistical background modeling technique to cope with a nonstationary camera. The current image is registered to the estimated background image using an affine or projective transformation. A mixture-of-Gaussians approach is then used to segment foreground objects from the background. Collins *et al.* [97] also discussed a background subtraction routine for a panning and tilting camera whereby the current image is registered using a projective transformation to one of many background images collected off line.

We stop at this point, though the discussion could range into many broad, widely studied computer vision topics such as segmentation [110], [111], tracking [35], and layered motion estimation [112], [113].

## IX. CHANGE MASK CONSISTENCY

The output of a change detection algorithm where decisions are made independently at each pixel will generally be noisy, with isolated change pixels, holes in the middle of connected change components, and jagged boundaries. Since changes in real image sequences often arise from the appearance or motion of solid objects in a specific size range with continuous, differentiable boundaries, most change detection algorithms try to conform the change mask to these expectations.

The simplest techniques simply postprocess the change mask with standard binary image processing operations, such as median filters, to remove small groups of pixels that differ from their neighbors' labels (salt and pepper noise) [114] or morphological operations [115] to smooth object boundaries.

Such approaches are less preferable than those that enforce spatial priors in the process of constructing the change mask. For example, Yamamoto [116] described a method in which an image sequence is collected into a 3-D stack, and regions of homogeneous intensity are unsupervisedly clustered. Changes are detected at region boundaries perpendicular to the temporal axis.

Most attempts to enforce consistency in change regions apply concepts from Markov–Gibbs random fields (MRFs), which are widely used in image segmentation. A standard technique is to apply a Bayesian approach where the prior probability of a given change mask is

$$P(B) = \frac{1}{Z} \exp^{-E(B)}$$

where  $Z$  is a normalization constant and  $E(B)$  is an energy term that is low when the regions in  $B$  exhibit smooth boundaries and high otherwise. For example, Aach *et al.* chose  $E(B)$  to be proportional to the number of label changes between four- and eight-connected neighbors in  $B$ . They discussed both an iterative method for a still image pair [74] and a noniterative method for an image sequence [75] for Bayesian change detection using such MRF priors. Bruzzone and Prieto [4], [69] used an MRF approach with a similar energy function. They maximized the *a posteriori* probability of the change mask using Besag's iterated conditional modes algorithm [117].

Instead of using a prior that influences the final change mask to be close to an MRF, Kasetkasem and Varshney [118] explicitly constrained the output change mask to be a valid MRF.

They proposed a simulated annealing algorithm [119] to search for the globally optimal change mask (i.e., the MAP estimate). However, they assumed that the inputs themselves were MRFs, which may be a reasonable assumption in terrain imagery, but less so for indoor surveillance imagery.

Finally, we note that some authors [102], [120] have taken an object-oriented approach to change detection, in which pixels are unsupervisedly clustered into homogeneously-textured objects *before* applying change detection algorithms. More generally, as stated in the introduction, there is a wide range of algorithms that use prior models for expected objects (e.g., buildings, cars, and people) to constrain the form of the objects in the detected change mask. Such scene understanding methods can be quite powerful, but are, perhaps, more accurately characterized as model-based segmentation and tracking algorithms than change detection.

## X. PRINCIPLES FOR PERFORMANCE EVALUATION AND COMPARISON

The performance of a change detection algorithm can be evaluated visually and quantitatively based on application needs. Subcomponents of change detection algorithms can also be evaluated individually. For example, Toyama *et al.* [88] gave a good overview of several background maintenance algorithms and provided a comparative example.

The most reliable approach for qualitative/visual evaluation is to display a flicker animation [121], a short movie file containing a registered pair of images ( $I_1(\mathbf{x})$ ,  $I_2(\mathbf{x})$ ) that are played in rapid succession at intervals of about a second each. In the absence of change, one perceives a steady image. When changes are present, the changed regions appear to flicker. The estimated change mask can also be superimposed on either image (e.g., as a semitransparent overlay, with different colors for different types of change).

Quantitative evaluation is more challenging, primarily due to the difficulty of establishing a valid “ground truth” or “gold standard.” This is the process of establishing the “correct answer” for what *exactly* the algorithm is expected to produce. A secondary challenge with quantitative validation is establishing the relative importance of different types of errors.

Arriving at the ground truth is an image analysis problem that is known to be difficult and time consuming [122]. Usually, the most appropriate source for ground truth data is an expert human observer. For example, a radiologist would be an appropriate expert human observer for algorithms performing change detection of X-ray images. As noted by Tan *et al.* [123], multiple-expert human observers can differ considerably, even when they are provided with a common set of guidelines. The same human observer can even generate different segmentations for the same data at two different times.

With the above-noted variability in mind, the algorithm designer may be faced with the need to establish ground truth from multiple conflicting observers [124]. A conservative method is to compare the algorithm against the set intersection of all human observers' segmentations. In other words, a change detected by the algorithm would be considered valid if every human observer considers it a change. A method that is less

susceptible to a single overly conservative observer is to use a majority rule. The least conservative approach is to compare the algorithm against the set union of all human observers' results. Finally, it is often possible to bring the observers together after an initial blind markup to develop a consensus markup.

Once a ground truth has been established, there are several standard methods for comparing the ground truth to a candidate binary change mask. The following quantities are generally involved:

- 1) true positives (TP): the number of change pixels correctly detected;
- 2) false positives (FP): the number of no-change pixels incorrectly detected as change (also known as false alarms);
- 3) true negatives (TN): the number of no-change pixels correctly detected;
- 4) false negatives (FN): the number of change pixels incorrectly detected as no-change (also known as misses).

Rosin [66] described three methods for quantifying a classifier's performance:

- 1) percentage correct classification  

$$PCC = (TP + TN) / (TP + FP + TN + FN);$$
- 2) Jaccard coefficient  

$$JC = TP / (TP + FP + FN);$$
- 3) Yule coefficient  

$$YC = |TP / (TP + FP) + TN / (TN + FN) - 1|.$$

For a classifier with tunable parameters, one can investigate the receiver-operating-characteristics (ROC) curve that plots the detection probability versus the false alarm probability to determine a desired level of performance. However, since an ROC curve gives little understanding of the qualitative behavior of a particular algorithm in different regions of the image pair, visual inspection of the change masks is still recommended.

Finally, we note that when there is an expected semantic interpretation of the changed pixels in a given application (e.g., an intruder in surveillance imagery), the algorithm designer should incorporate higher level constraints that reflect the ability of a given algorithm to detect the "most important" changes, instead of treating every pixel equally.

## XI. CONCLUSIONS AND DISCUSSION

The two application domains that have seen the most activity in change detection algorithms are remote sensing and video surveillance, and their approaches to the problem are often quite different. We have attempted to survey the recent state of the art in image change detection without emphasizing a particular application area. We hope that our classification of algorithms into a relatively small number of categories will provide useful guidance to the algorithm designer. We note there are several software packages that include some of the change detection algorithms discussed here (e.g., [125], [126]). In particular, we have developed a companion website to this paper [127] that includes implementations, results, and comparative analysis of several of the methods discussed above. Color versions of Figs. 1 and 2 are also available on this website.

We have tried not to over editorialize regarding the relative merits of the algorithms, leaving the reader to decide which assumptions and constraints may be most relevant for his or

her application. However, our opinion is that two algorithms deserve special mention. Stauffer and Grimson's background modeling algorithm [2], covered in Section VIII, provides for multiple models of background appearance as well as object appearance and motion. The algorithm by Black *et al.* [80], covered in Section V-C, provides for multiple models of image change and requires no preprocessing to compensate for misregistration or illumination variation. We expect that a combination of these approaches that uses soft assignment of each pixel to an object class and one or more change models would produce a very general, powerful, and theoretically well-justified change detection algorithm.

Despite the substantial amount of work in the field, change detection is still an active and interesting area of research. We expect future algorithm developments to be fueled by increasingly more integrated approaches combining elaborate models of change, implicit pre- and post-processing, robust statistics, and global optimization methods. We also expect future developments to leverage progress in the related areas of computer vision research (e.g., segmentation, tracking, motion estimation, and structure-from-motion) mentioned in the text. Finally, and, perhaps, most importantly, we expect a continued growth of societal applications of change detection and interpretation in key areas such as biotechnology and geospatial intelligence.

## ACKNOWLEDGMENT

The authors would like to thank the anonymous reviewers and associate editors for their insightful comments that helped improve the quality of this work. They would also like to thank Dr. A. Majerovics at the Center for Sight, Albany, NY for the images in Fig. 2.

## REFERENCES

- [1] R. Collins, A. Lipton, and T. Kanade, "Introduction to the special section on video surveillance," *IEEE Trans. Pattern Anal. Mach. Intell.*, vol. 22, no. 8, pp. 745–746, Aug. 2000.
- [2] C. Stauffer and W. E. L. Grimson, "Learning patterns of activity using real-time tracking," *IEEE Trans. Pattern Anal. Mach. Intell.*, vol. 22, no. 8, pp. 747–757, Aug. 2000.
- [3] C. R. Wren, A. Azarbayejani, T. Darrell, and A. Pentland, "Pfinder: Real-time tracking of the human body," *IEEE Trans. Pattern Anal. Mach. Intell.*, vol. 19, no. 7, pp. 780–785, Jul. 1997.
- [4] L. Bruzzone and D. F. Prieto, "An adaptive semiparametric and context-based approach to unsupervised change detection in multitemporal remote-sensing images," *IEEE Trans. Image Processing*, vol. 11, no. 4, pp. 452–466, Apr. 2002.
- [5] J. B. Collins and C. E. Woodcock, "An assessment of several linear change detection techniques for mapping forest mortality using multi-temporal Landsat TM data," *Remote Sens. Environ.*, vol. 56, pp. 66–77, 1996.
- [6] A. Huertas and R. Nevatia, "Detecting changes in aerial views of man-made structures," *Image Vis. Comput.*, vol. 18, no. 8, pp. 583–596, May 2000.
- [7] M. Bosc, F. Heitz, J. P. Armspach, I. Namer, D. Gounot, and L. Rumbach, "Automatic change detection in multimodal serial MRI: Application to multiple sclerosis lesion evolution," *Neuroimage*, vol. 20, pp. 643–656, 2003.
- [8] M. J. Dumskyj, S. J. Aldington, C. J. Dore, and E. M. Kohner, "The accurate assessment of changes in retinal vessel diameter using multiple frame electrocardiograph synchronised fundus photography," *Current Eye Res.*, vol. 15, no. 6, pp. 652–632, Jun. 1996.
- [9] L. Lemieux, U. Wiesmann, N. Moran, D. Fish, and S. Shorvon, "The detection and significance of subtle changes in mixed-signal brain lesions by serial MRI scan matching and spatial normalization," *Med. Image Anal.*, vol. 2, no. 3, pp. 227–242, 1998.

- [10] D. Rey, G. Subsol, H. Delingette, and N. Ayache, "Automatic detection and segmentation of evolving processes in 3D medical images: Application to multiple sclerosis," *Med. Image Anal.*, vol. 6, no. 2, pp. 163–179, Jun. 2002.
- [11] J.-P. Thirion and G. Calmon, "Deformation analysis to detect and quantify active lesions in three-dimensional medical image sequences," *IEEE Trans. Med. Imag.*, vol. 18, no. 5, pp. 429–441, May 1999.
- [12] E. Landis, E. Nagy, D. Keane, and G. Nagy, "A technique to measure 3D work-of-fracture of concrete in compression," *J. Eng. Mech.*, vol. 126, no. 6, pp. 599–605, Jun. 1999.
- [13] G. Nagy, T. Zhang, W. Franklin, E. Landis, E. Nagy, and D. Keane, "Volume and surface area distributions of cracks in concrete," in *Proc. Visual Form*, 2001, pp. 759–768.
- [14] D. Edgington, W. Dirk, K. Salamy, C. Koch, M. Risi, and R. Sherlock, "Automated event detection in underwater video," in *Proc. MTS/IEEE Oceans Conf.*, 2003.
- [15] K. Lebart, E. Trucco, and D. M. Lane, "Real-time automatic sea-floor change detection from video," in *Proc. MTS/IEEE OCEANS*, Sep. 2000, pp. 337–343.
- [16] J. Whorff and L. Griffing, "A video recording and analysis system used to sample intertidal communities," *J. Exp. Marine Biol. Ecol.*, vol. 160, pp. 1–12, 1992.
- [17] C.-Y. Fang, S.-W. Chen, and C.-S. Fuh, "Automatic change detection of driving environments in a vision-based driver assistance system," *IEEE Trans. Neural Netw.*, vol. 14, no. 3, pp. 646–657, May 2003.
- [18] W. Y. Kan, J. V. Krogmeier, and P. C. Doerschuk, "Model-based vehicle tracking from image sequences with an application to road surveillance," *Opt. Eng.*, vol. 35, no. 6, pp. 1723–1729, 1996.
- [19] A. Singh, "Digital change detection techniques using remotely-sensed data," *Int. J. Remote Sens.*, vol. 10, no. 6, pp. 989–1003, 1989.
- [20] P. Coppin and M. Bauer, "Digital change detection in forest ecosystems with remote sensing imagery," *Remote Sens. Rev.*, vol. 13, pp. 207–234, 1996.
- [21] S. Watanabe, K. Miyajima, and N. Mukawa, "Detecting changes of buildings from aerial images using shadow and shading model," in *Proc. ICPR*, 1998, pp. 1408–1412.
- [22] P. Deer and P. Eklund, "Values for the fuzzy C-means classifier in change detection for remote sensing," in *Proc. 9th Int. Conf. Information Processing and Management of Uncertainty*, 2002, pp. 187–194.
- [23] L. Bruzzone and S. Serpico, "An iterative technique for the detection of land-cover transitions in multitemporal remote-sensing images," *IEEE Trans. Geosci. Remote Sens.*, vol. 35, no. 4, pp. 858–867, Jul. 1997.
- [24] F. Gustafsson, *Adaptive Filtering and Change Detection*. New York: Wiley, 2000.
- [25] M. Yeung, B. Yeo, and B. Liu, "Segmentation of video by clustering and graph analysis," *Comput. Vis. Image Understanding*, vol. 71, no. 1, pp. 94–109, Jul. 1998.
- [26] H. Yu and W. Wolf, "A hierarchical multiresolution video shot transition detection scheme," *Comput. Vis. Image Understanding*, vol. 75, no. 1/2, pp. 196–213, Jul. 1999.
- [27] L. G. Brown, "A survey of image registration techniques," *ACM Comput. Surv.*, vol. 24, no. 4, 1992.
- [28] S. Lavallee, *Registration for Computer-Integrated Surgery: Methodology, State of the Art*. Cambridge, MA: MIT Press, 1995.
- [29] J. B. A. Maintz and M. A. Viergever, "A survey of medical image registration," *Med. Image Anal.*, vol. 2, no. 1, pp. 1–36, 1998.
- [30] B. Zitová and J. Flusser, "Image registration methods: A survey," *Image Vis. Comput.*, vol. 21, pp. 977–1000, 2003.
- [31] L. Ibáñez, W. Schroeder, L. Ng, and J. Cates, *The ITK Software Guide: The Insight Segmentation and Registration Toolkit*, 1.4 ed: Kitware, Inc., 2003.
- [32] A. Can, C. V. Stewart, B. Roysam, and H. L. Tanenbaum, "A feature-based, robust, hierarchical algorithm for registering pairs of images of the curved human retina," *IEEE Trans. Pattern Anal. Mach. Intell.*, vol. 24, no. 3, pp. 347–364, Mar. 2002.
- [33] C. V. Stewart, C.-L. Tsai, and B. Roysam, "The dual-bootstrap iterative closest point algorithm with application to retinal image registration," *IEEE Trans. Med. Imag.*, vol. 22, no. 11, pp. 1379–1394, Nov. 2003.
- [34] J. Barron, D. Fleet, and S. Beauchemin, "Performance of optical flow techniques," *Int. J. Comput. Vis.*, vol. 12, no. 1, pp. 43–77, 1994.
- [35] A. Blake and M. Isard, *Active Contours*. New York: Springer-Verlag, 1999.
- [36] D. G. Lowe, "Distinctive image features from scale-invariant keypoints," *Int. J. Comput. Vis.*, vol. 60, no. 2, pp. 91–110, 2004.
- [37] W. Wells, "Statistical approaches to feature-based object recognition," *Int. J. Comput. Vis.*, vol. 21, no. 1/2, pp. 63–98, 1997.
- [38] D. Forsyth and J. Ponce, *Computer Vision: A Modern Approach*. Upper Saddle River, NJ: Prentice-Hall, 2003.
- [39] R. Hartley and A. Zisserman, *Multiple View Geometry in Computer Vision*. Cambridge, U.K.: Cambridge Univ. Press, 2000.
- [40] D. A. Stow, "Reducing the effects of misregistration on pixel-level change detection," *Int. J. Remote Sens.*, vol. 20, no. 12, pp. 2477–2483, 1999.
- [41] J. Townshend, C. Justice, C. Gurney, and J. McManus, "The impact of misregistration on change detection," *IEEE Trans. Geosci. Remote Sens.*, vol. 30, no. 5, pp. 1054–1060, Sep. 1992.
- [42] X. Dai and S. Khorram, "The effects of image misregistration on the accuracy of remotely sensed change detection," *IEEE Trans. Geosci. Remote Sens.*, vol. 36, no. 5, pp. 1566–1577, Sep. 1998.
- [43] L. Bruzzone and R. Cossu, "An adaptive approach to reducing registration noise effects in unsupervised change detection," *IEEE Trans. Geosci. Remote Sens.*, vol. 41, no. 6, pp. 2455–2465, Nov. 2003.
- [44] R. Lillestrand, "Techniques for change detection," *IEEE Trans. Comput.*, vol. 21, no. 7, pp. 654–659, Jul. 1972.
- [45] M. S. Ulstad, "An algorithm for estimating small scale differences between two digital images," *Pattern Recognit.*, vol. 5, pp. 323–333, 1973.
- [46] B. Phong, "Illumination for computer generated pictures," *Commun. ACM*, vol. 18, pp. 311–317, 1975.
- [47] T. A. D. Lath and V. Metzler, "Illumination-invariant change detection," in *Proc. 4th IEEE Southwest Symp. Image Analysis and Interpretation*, Apr. 2000, pp. 3–7.
- [48] T. Aach, L. Dümbgen, R. Mester, and D. Toth, "Bayesian illumination-invariant motion detection," in *Proc. IEEE Int. Conf. Image Processing*, Oct. 2001, pp. 640–643.
- [49] O. Pizarro and H. Singh, "Toward large-area mosaicing for underwater scientific applications," *IEEE J. Ocean. Eng.*, vol. 28, no. 4, pp. 651–672, Oct. 2003.
- [50] S. Negahdaripour, "Revised definition of optical flow: Integration of radiometric and geometric cues for dynamic scene analysis," *IEEE Trans. Pattern Anal. Mach. Intell.*, vol. 20, no. 9, pp. 961–979, Sep. 1998.
- [51] G. D. Hager and P. N. Belhumeur, "Efficient region tracking with parametric models of geometry and illumination," *IEEE Trans. Pattern Anal. Mach. Intell.*, vol. 20, no. 10, pp. 1025–1039, Oct. 1998.
- [52] P. Bromiley, N. Thacker, and P. Courtney, "Non-parametric image subtraction using grey level scattergrams," *Image Vis. Comput.*, vol. 20, no. 9–10, pp. 609–617, Aug. 2002.
- [53] P. Viola, "Alignment by maximization of mutual information," *Int. J. Comput. Vis.*, vol. 24, no. 2, pp. 137–154, Sep. 1997.
- [54] J. Jensen, *Introductory Digital Image Processing, a Remote Sensing Perspective*. Upper Saddle River, NJ: Prentice-Hall, 1996.
- [55] I. Niemeyer, M. Canty, and D. Klaus, "Unsupervised change detection techniques using multispectral satellite images," in *Proc. IEEE Int. Geo-science and Remote Sensing Symp.*, Jul. 1999, pp. 327–329.
- [56] P. Gong, "Change detection using principal components analysis and fuzzy set theory," *Canad. J. Remote Sens.*, vol. 19, Jan. 1993.
- [57] E. P. Crist and R. C. Cicone, "A physically-based transformation of Thematic Mapper data – The TM tasseled cap," *IEEE Trans. Geosci. Remote Sens.*, vol. 22, no. 2, pp. 256–263, Mar. 1984.
- [58] J. Morissette and S. Khorram, "An introduction to using generalized linear models to enhance satellite-based change detection," in *Proc. IGARSS*, vol. 4, 1997, pp. 1769–1771.
- [59] A. Elgammal, R. Duraiswami, D. Harwood, and L. S. Davis, "Background and foreground modeling using nonparametric kernel density estimation for visual surveillance," *Proc. IEEE*, vol. 90, no. 7, pp. 1151–1163, Jul. 2002.
- [60] B. Xie, V. Ramesh, and T. Boulton, "Sudden illumination change detection using order consistency," *Image Vis. Comput.*, vol. 22, no. 2, pp. 117–125, Feb. 2004.
- [61] L. M. T. Carvalho, L. M. G. Fonseca, F. Murtagh, and J. G. P. W. Clevers, "Digital change detection with the aid of multi-resolution wavelet analysis," *Int. J. Remote Sens.*, vol. 22, no. 18, pp. 3871–3876, 2001.
- [62] S. Fukuda and H. Hirose, "Suppression of speckle in synthetic aperture radar images using wavelet," *Int. J. Remote Sens.*, vol. 19, no. 3, pp. 507–519, 1998.
- [63] S. Quegan and J. Schou, "The principles of polarimetric filtering," in *Proc. IGARSS*, Aug. 1997, pp. 1041–1043.
- [64] R. Touzi, "A review of speckle filtering in the context of estimation theory," *IEEE Trans. Geosci. Remote Sens.*, vol. 40, no. 6, pp. 2392–2404, Nov. 2002.
- [65] P. Rosin, "Thresholding for change detection," *Comput. Vis. Image Understanding*, vol. 86, no. 2, pp. 79–95, May 2002.

- [66] P. Rosin and E. Ioannidis, "Evaluation of global image thresholding for change detection," *Pattern Recognit. Lett.*, vol. 24, no. 14, pp. 2345–2356, Oct. 2003.
- [67] P. Smits and A. Annoni, "Toward specification-driven change detection," *IEEE Trans. Geosci. Remote Sens.*, vol. 38, no. 3, pp. 1484–1488, May 2000.
- [68] H. V. Poor, *An Introduction to Signal Detection and Estimation*, 2nd ed. New York: Springer-Verlag, 1994.
- [69] L. Bruzzone and D. F. Prieto, "Automatic analysis of the difference image for unsupervised change detection," *IEEE Trans. Geosci. Remote Sens.*, vol. 38, no. 3, pp. 1171–1182, May 2000.
- [70] J. E. Colwell and F. P. Weber, "Forest change detection," in *Proc. 15th Int. Symp. Remote Sensing of Environment*, 1981, pp. 839–852.
- [71] W. A. Malila, "Change vector analysis: An approach for detecting forest changes with Landsat," in *Proc. 6th Annu. Symp. Machine Processing of Remotely Sensed Data*, 1980, pp. 326–335.
- [72] L. di Stefano, S. Mattoccia, and M. Mola, "A change-detection algorithm based on structure and color," in *Proc. IEEE Conf. Advanced Video and Signal-Based Surveillance*, 2003, pp. 252–259.
- [73] S. M. Kay, *Fundamentals of Statistical Signal Processing: Detection Theory*. Upper Saddle River, NJ: Prentice-Hall, 1993.
- [74] T. Aach and A. Kaup, "Statistical model-based change detection in moving video," *Signal Process.*, vol. 31, pp. 165–180, Mar. 1993.
- [75] —, "Bayesian algorithms for adaptive change detection in image sequences using Markov random fields," *Signal Process.: Image Commun.*, vol. 7, pp. 147–160, Aug. 1995.
- [76] R. Thoma and M. Bierling, "Motion compensating interpolation considering covered and uncovered background," *Signal Process.: Image Commun.*, vol. 1, no. 2, pp. 191–212, Oct. 1989.
- [77] E. Rignot and J. van Zyl, "Change detection techniques for ERS-1 SAR data," *IEEE Trans. Geosci. Remote Sens.*, vol. 31, no. 4, pp. 896–906, Jul. 1993.
- [78] A. P. Dempster, N. M. Laird, and D. B. Rubin, "Maximum likelihood from incomplete data via the EM algorithm," *J. Roy. Stat. Soc.*, vol. 39, no. 1, pp. 1–38, 1977.
- [79] K. Fukunaga and R. Hayes, "The reduced Parzen classifier," *IEEE Trans. Pattern Anal. Mach. Intell.*, vol. 11, no. 4, pp. 423–425, Apr. 1989.
- [80] M. J. Black, D. J. Fleet, and Y. Yacoob, "Robustly estimating changes in image appearance," *Comput. Vis. Image Understanding*, vol. 78, no. 1, pp. 8–31, 2000.
- [81] Y. G. Leclerc, Q.-T. Luong, and P. V. Fua, "Self-consistency and MDL: A paradigm for evaluating point-correspondence algorithms, and its application to detecting changes in surface elevation," *Int. J. Comput. Vis.*, vol. 51, no. 1, pp. 63–83, Jan. 2003.
- [82] J. Rissanen, "Minimum-description-length principle," in *Encyclopedia of Statistical Sciences*, 5th ed. New York: Wiley, 1987, pp. 523–527.
- [83] Y. Z. Hsu, H.-H. Nagel, and G. Reckers, "New likelihood test methods for change detection in image sequences," *Comput. Vis., Graph. Image Process.*, vol. 26, pp. 73–106, 1984.
- [84] Y. Yakimovsky, "Boundary and object detection in real world images," *J. ACM*, vol. 23, no. 4, pp. 599–618, Oct. 1976.
- [85] K. Skifstad and R. Jain, "Illumination independent change detection for real world image sequences," *Comput. Vis. Graph. Image Process.*, vol. 46, no. 3, pp. 387–399, 1989.
- [86] A. Elfishawy, S. Kesler, and A. Abutaleb, "Adaptive algorithms for change detection in image sequence," *Signal Process.*, vol. 23, no. 2, pp. 179–191, 1991.
- [87] Z. Jain and Y. Chau, "Optimum multisensor data fusion for image change detection," *IEEE Trans. Syst., Man, Cybern.*, vol. 25, no. 9, pp. 1340–1347, Sep. 1995.
- [88] K. Toyama, J. Krumm, B. Brumitt, and B. Meyers, "Wallflower: Principles and practice of background maintenance," in *Proc. ICCV*, 1999, pp. 255–261.
- [89] M. Carlotto, "Detection and analysis of change in remotely sensed imagery with application to wide area surveillance," *IEEE Trans. Image Process.*, vol. 6, no. 1, pp. 189–202, Jan. 1997.
- [90] C. Clifton, "Change detection in overhead imagery using neural networks," *Appl. Intell.*, vol. 18, pp. 215–234, 2003.
- [91] E. Durucan and T. Ebrahimi, "Change detection and background extraction by linear algebra," *Proc. IEEE*, vol. 89, no. 10, pp. 1368–1381, Oct. 2001.
- [92] —, "Change detection by nonlinear Grammian," in *Proc. NSIP*, Sep. 2001.
- [93] H. Anton and C. Rorres, *Elementary Linear Algebra*. New York: Wiley, 1994.
- [94] R. Mester, T. Aach, and L. Dumbgen, "Illumination-invariant change detection using a statistical colinearity criterion," in *Proc. 23rd DAGM Symp.*, Sep. 2001, pp. 170–177.
- [95] L. Li and M. K. H. Leung, "Integrating intensity and texture differences for robust change detection," *IEEE Trans. Image Process.*, vol. 11, pp. 105–112, Feb. 2002.
- [96] S. Liu, C. Fu, and S. Chang, "Statistical change detection with moments under time-varying illumination," *IEEE Trans. Image Process.*, vol. 7, pp. 1258–1268, Sep. 1998.
- [97] R. Collins, A. Lipton, T. Kanade, H. Fujiyoshi, D. Duggins, Y. Tsin, D. Tolliver, N. Enomoto, and O. Hasegawa, "A system for video surveillance and monitoring," Robotics Inst., Carnegie-Mellon Univ., Pittsburgh, PA, Tech. Rep. CMU-RI-TR-00-12, 2000.
- [98] A. Cavallaro and T. Ebrahimi, "Video object extraction based on adaptive background and statistical change detection," in *Proc. SPIE Visual Communications and Image Processing*, Jan. 2001, pp. 465–475.
- [99] S. Huwer and H. Niemann, "Adaptive change detection for real-time surveillance applications," in *Proc. Visual Surveillance*, 2000.
- [100] T. Kanade, R. Collins, A. Lipton, P. Burt, and L. Wixson, "Advances in cooperative multi-sensor video surveillance," in *Proc. DARPA Image Understanding Workshop*, vol. 1, Nov. 1998, pp. 3–24.
- [101] D. Gibbins, G. N. Newsam, and M. J. Brooks, "Detecting suspicious background changes in video surveillance of busy scenes," in *Proc. 3rd IEEE Workshop on Applications in Computer Vision*, Dec. 1996, pp. 22–26.
- [102] M. Höttner, R. Mester, and M. Meyer, "Detection of moving objects using a robust displacement estimation including a statistical error analysis," in *Proc. Int. Conf. Pattern Recognition*, 1996, pp. 249–255.
- [103] N. Paragios and G. Tziritas, "Adaptive detection and localization of moving objects in image sequences," *Signal Process.: Image Commun.*, vol. 14, no. 4, pp. 277–296, Jan. 1999.
- [104] J. Rittscher, J. Kato, S. Joga, and A. Blake, "A probabilistic background model for tracking," in *Proc. 6th ECCV*, 2000.
- [105] B. Stenger, R. Visvanathan, N. Paragios, F. Coetzee, and J. Buhmann, "Topology free hidden Markov models: Applications to background modeling," in *Proc. IEEE Int. Conf. Computer Vision*, Jul. 2001, pp. 294–301.
- [106] I. Haritaoglu, D. Harwood, and L. S. Davis, "W4: Real-time surveillance of people and their activities," *IEEE Trans. Pattern Anal. Mach. Intell.*, vol. 22, no. 8, pp. 809–830, Aug. 2000.
- [107] Y. Ivanov, A. Bobick, and J. Liu, "Fast lighting independent background subtraction," *Int. J. Comput. Vis.*, vol. 37, no. 2, pp. 199–207, Jun. 2000.
- [108] L. J. Latecki, X. Wen, and N. Ghubade, "Detection of changes in surveillance videos," in *Proc. IEEE Int. Conf. Advanced Video and Signal Based Surveillance*, Jul. 2003, pp. 237–242.
- [109] Y. Ren, C. Chua, and Y. Ho, "Statistical background modeling for nonstationary camera," *Pattern Recognit. Lett.*, vol. 24, no. 1–3, pp. 183–196, Jan. 2003.
- [110] S. Z. Li, *Markov Random Field Modeling in Image Analysis*, 2nd ed. New York: Springer-Verlag, 2001.
- [111] N. Pal and S. Pal, "A review on image segmentation techniques," *Pattern Recognit.*, vol. 26, no. 9, pp. 1277–1294, 1993.
- [112] S. Ayer and H. Sawhney, "Layered representation of motion video using robust maximum-likelihood estimation of mixture models and MDL encoding," in *Proc. ICCV*, Jun. 1995.
- [113] J. Wang and E. Adelson, "Representing moving objects with layers," *IEEE Trans. Image Process.*, vol. 3, no. 9, pp. 625–638, Sep. 1994.
- [114] R. M. Haralick and L. G. Shapiro, *Computer and Robot Vision*. Reading, MA: Addison-Wesley, 1992, vol. 1.
- [115] E. Stringa, "Morphological change detection algorithms for surveillance applications," in *Proc. Brit. Machine Vision Conf.*, 2000.
- [116] T. Yamamoto, H. Hanaizumi, and S. Chino, "A change detection method for remotely sensed multispectral and multitemporal images using 3-D segmentation," *IEEE Trans. Geosci. Remote Sens.*, vol. 39, no. 3, pp. 976–985, May 2001.
- [117] J. Besag, "On the statistical analysis of dirty pictures," *J. Roy. Stat. Soc. B*, vol. 48, pp. 259–302, 1986.
- [118] T. Kasetskam and P. Varshney, "An image change detection algorithm based on Markov random field models," *IEEE Trans. Geosci. Remote Sens.*, vol. 40, no. 4, pp. 1815–1823, Jul. 2002.
- [119] S. Geman and D. Geman, "Stochastic relaxation, Gibbs distributions, and the Bayesian restoration of images," *IEEE Trans. Pattern Anal. Mach. Intell.*, vol. 6, no. 6, pp. 721–741, 1984.
- [120] O. Hall and G. Hay, "A multi-scale object-specific approach to digital change detection," *Int. J. Appl. Earth Observation Geoinf.*, vol. 4, no. 4, pp. 311–327, 2003.

- [121] J. W. Berger, T. R. Patel, D. S. Shin, J. R. Piltz, and R. A. Stone, "Computerized stereochronoscopy and alteration flicker to detect optic nerve head contour change," *Ophthalmol.*, vol. 107, no. 7, Jul. 2000.
- [122] J. Hu, R. Kahsi, D. Lopresti, G. Nagy, and G. Wilfong, "Why table ground-truthing is hard," in *Proc. 6th Int. Conf. Document Analysis and Recognition*, 2001, pp. 129–133.
- [123] I. L. Tan, R. van Schijndel, F. Fazekas, M. Filippi, P. Freitag, D. H. Miller, T. A. Yousry, P. J. W. Pouwels, H. J. Ader, and F. Barkhof, "Image registration and subtraction to detect active  $T_2$  lesions in MS: An inter-observer study," *J. Neurol.*, vol. 249, pp. 767–773, 2002.
- [124] K. H. Fritzsche, A. Can, H. Shen, C.-L. Tsai, J. N. Turner, H. L. Tanenbaum, C. V. Stewart, and B. Roysam, "Automated model-based segmentation, tracing, and analysis of retinal vasculature from digital fundus images," in *Angiography and Plaque Imaging: Advanced Segmentation Techniques*. Boca Raton, FL: CRC, 2003, pp. 225–297.
- [125] Adaptive Terrain Change Analysis (ATCA) Software. Applied Analysis, Inc., Billerica, MA. [Online]. Available: <http://www.discover-aai.com/software/products/ATCA.htm>
- [126] Environment for Visualizing Images (ENVI) Software. Research Systems, Inc., Boulder, CO. [Online]. Available: <http://www.rsinc.com/envi/index.cfm>
- [127] S. Andra and O. Al-Kofahi. (2004) Matlab Change Detection Suite. Rensselaer Polytech. Inst., Troy, NY. [Online]. Available: <http://www.ecse.rpi.edu/censsis/papers/change/>



**Richard J. Radke** (S'98–M'01) received the B.A. degree in mathematics and the B.A. and M.A. degrees in computational and applied mathematics from Rice University, Houston, TX, in 1996, and the Ph.D. degree from the Electrical Engineering Department, Princeton University, Princeton, NJ, in 2001. For his Ph.D. research, he investigated several estimation problems in digital video, including the synthesis of photorealistic "virtual video" in collaboration with IBM's Tokyo Research Laboratory, and he also interned at the Mathworks, Inc., Natick, MA,

developing numerical linear algebra and signal processing routines.

He joined the faculty of the Department of Electrical, Computer, and Systems Engineering, Rensselaer Polytechnic Institute, Troy, NY, in August, 2001, where he is also associated with the National Science Foundation Engineering Research Center for Subsurface Sensing and Imaging Systems (CenSSIS). His current research interests include distributed computer vision problems on large camera networks, deformable registration and segmentation of three- and four-dimensional biomedical volumes, and 3-D modeling and tracking from distributed mobile sensors.

Dr. Radke received a National Science Foundation CAREER Award in 2003.



**Srinivas Andra** (S'04) received the B.Tech. degree in electronics and communication engineering from the National Institute of Technology, Warangal, India, and the M.S. degree in electrical engineering from Rensselaer Polytechnic Institute (RPI), Troy, NY, in 1999 and 2003, respectively. He is currently pursuing the Ph.D. degree at RPI.

His research interests include machine learning, particularly support vector machines and kernel methods, pattern recognition, and image processing.



**Omar Al-Kofahi** (S'03) received the B.S. degree in electrical, computer, and systems engineering from the Jordan University of Science and Technology, Jordan, and the M.S. degree in electrical, computer, and systems engineering from Rensselaer Polytechnic Institute (RPI), Troy, NY, in 1998 and 2001, respectively. He is currently pursuing the Ph.D. degree in the Electrical, Computer, and Systems Engineering Department, RPI.

He was a System Administrator for Zeine Technological Applications in Jordan from 1998 to 2000, where he earned several professional certificates as a System Administrator. Since joining RPI in 2000, he has been an active student member of the National Science Foundation Center for Subsurface Sensing and Imaging Systems (CenSSIS), where he served as the President for the Student Leadership Council. His research is focused on multidimensional biomedical image enhancement and analysis and image-change detection and understanding.



**Badrinath Roysam** (M'89) received the B.Tech. degree in electronics engineering from the Indian Institute of Technology, Madras, and the M.S. and D.Sc. degrees from Washington University, St. Louis, MO, in 1984, 1987, and 1989, respectively.

He has been with Rensselaer Polytechnic Institute, Troy, NY, since 1989, where he is currently a Professor in the Electrical, Computer, and Systems Engineering Department. He is an Associate Director of the Center for Subsurface Sensing and Imaging Systems (CenSSIS)—a multiuniversity,

National Science Foundation-sponsored engineering research center, where he also holds an appointment in the Biomedical Engineering Department. His ongoing projects are in the areas of multidimensional biomedical image analysis, biotechnology automation, optical instrumentation, high-speed and real-time computing architectures, and parallel algorithms.

Dr. Roysam is a member of the ASEE, the Microscopy Society of America, the Society for Neuroscience, the Society for Molecular Imaging, and the Association for Research in Vision and Ophthalmology. He is an Associate Editor for the IEEE TRANSACTIONS ON INFORMATION THEORY in biomedicine.